Insulin induces cation fluxes and increases intracellular calcium in the HTC rat hepatoma cell line

Laurence Mathé PhD[1], Diane Vallerand BSc[1], Pierre S Haddad PhD[1,2]

L Mathé, D Vallerand, P Haddad. Insulin induces cation fluxes and increases intracellular calcium in the HTC rat hepatoma cell line. Can J Gastroenterol 2000;14(5):389-396.

BACKGROUND/AIMS: Rat hepatoma HTC cells were used to study conductive pathways implicated in insulin-induced cation and calcium influx into liver cells.
METHODS: Membrane potentials and currents were measured by whole-cell patch clamp. Cytosolic calcium was measured using FURA-2 fluorescence.
RESULTS: Insulin induced a gradual and reversible depolarization of 5.7±0.8 mV. Insulin-induced currents showed a linear slope conductance of 663 pS and a reversal potential of –17.9 mV. Ion substitution experiments showed that these currents were composed mainly of a nonselective cation component. In FURA-2 experiments, insulin caused a slow monophasic rise in HTC cell calcium, which depended on the presence of extracellular calcium. Insulin also induced significant increases of 1.58- and 1.54-fold in basal calcium influx when studied by external calcium withdrawal and readmission, or by the manganese quench method, respectively. Using the latter approach, we found that 100 µM gadolinium and 10 µM SKF96365 blocked the rise of the basal manganese quench rate induced by insulin whereas 100 µM verapamil was without effect.
CONCLUSIONS: Insulin induces inward cation currents that depolarize HTC cell membrane potentials and participate in increased calcium influx.

Key Words: *Fura-2; Hepatocytes; Nonselective cation channels; Patch clamping*

L'insuline déclenche des flux de cations et augmente le calcium intracellulaire dans la lignée cellulaire d'hépatome du rat HTC

HISTORIQUE-OBJECTIFS : On a utilisé des cellules HTC d'hépatome du rat pour étudier les voies de conduction impliquées dans l'influx de calcium et de cations déclenché par l'insuline dans les hépatocytes.
MÉTHODES : On a mesuré les potentiels et les courants membranaires par la technique du « patch-clamp » à cellule entière. On a aussi mesuré le calcium cytosolique par la technique de fluorescence FURA-2.
RÉSULTATS : L'insuline a déclenché une dépolarisation graduelle et réversible de 5,7 ± 0,8 mV. Les courants déclenchés par l'insuline ont fait apparaître une conductance à pente linéaire de 663 pS et un potentiel d'inversion de - 17,9 mV. Les expériences de substitution des ions ont démontré que ces courants étaient principalement composés de cations non sélectionnés. Dans les expériences utilisant la fluorescence FURA-2, l'insuline a entraîné une augmentation monophasique lente du calcium des HTC, qui dépendait de la présence de calcium extracellulaire. L'insuline a déclenché des augmentations significatives de 1,58 et 1,54 fois de l'influx de base de calcium lorsque étudiée respectivement par la méthode de réadmission ou de retrait du calcium externe, ou bien par la technique de l'extinction de fluorescence du manganèse. En utilisant cette dernière méthode, on a mis en évidence que 100 µM de gadolinium et 10 µM de SKF96365 bloquaient l'augmentation du taux basal d'extinction du manganèse déclenchée par l'insuline alors que 100 µM de vérapamil n'entraînait aucun effet.
CONCLUSIONS : L'insuline déclenche des flux entrants de cations qui dépolarisent les potentiels membranaires des cellules HTC et participent à l'augmentation de l'influx de calcium.

Groupe de Recherche en Transport Membranaire et Départements de [1]pharmacologie et de [2]physiologie, Université de Montréal, Montréal, Québec
Correspondence and reprints: Dr PS Haddad, Département de pharmacologie, Université de Montréal, CP 6128, Succursale Centre-Ville, Montréal Quebec H3C 3J7. Telephone 514-343-6590, fax 514-343-2291, e-mail Pierre.Haddad@umontreal.ca
Received for publication January 5, 2000. Accepted March 20, 2000

Cell surface tyrosine kinase-linked receptors mediate the cellular response to certain hormones, with insulin being a common example (1). In liver cells, the primary physiological role of insulin is to participate in the control of carbohydrate, lipid and protein metabolism (2,3). In addition, insulin induces a slow depolarization of membrane potential in primary cultured rat hepatocytes (4) and antagonizes glucagon-evoked hyperpolarization in the isolated perfused rat liver (5). Insulin also promotes cation influx into liver cells by unspecified mechanisms, and this effect is important for its metabolic actions (6). The action of insulin on cytosolic calcium, on the other hand, is more controversial. The hormone increases cytosolic calcium in vascular smooth muscle cells (7) and has no effect on intracellular calcium in a skeletal muscle cell line (8), whereas contradictory results have been reported in adipocytes (9,10). Finally, recent results from our laboratory have shown that insulin increases steady state intracellular calcium in primary cultured rat hepatocytes by promoting an influx of the ion from the extracellular milieu (11). However, the mechanisms by which insulin triggers membrane potential change and calcium influx in liver cells remain unclear.

The pathway(s) of calcium entry into liver cells is still an area of active investigation. In hepatocytes, there is no evidence for the presence of voltage-activated calcium channels, whether by functional experiments (12) or at the mRNA level (13). Recent studies have demonstrated the presence of nonselective cation channels (NSCC) on the surface of isolated rat hepatocytes and of the HTC model liver cell line (14). The channels exhibit slope conductances of 18 and 28 pS, can use sodium, potassium or calcium ions equally well as charge carriers, and their open probability depends on the cytosolic calcium concentration but not on membrane voltage (14,15). Under physiological conditions, these channels are thought to mediate largely sodium and calcium influx into liver cells (14). A previous report (16) using HTC cells also demonstrated that NSCCs are inhibited by nickel and SKF96365 but not by verapamil, properties that correspond to store depletion-triggered calcium influx in primary rat hepatocytes (17). However, the conductive pathways responsible for the cation influx induced by insulin into liver cells have not been explored.

The present study aimed to determine the mechanisms by which insulin modulates hepatocellular electrophysiological membrane properties and influences intracellular calcium.

MATERIALS AND METHODS

Cell culture: Rat hepatoma HTC cells were chosen because they express surface membrane channels very similar to those found in primary cultures of rat hepatocytes while offering a greater stability for measurements of membrane currents by the patch clamp method (14). HTC cells were provided by Dr J Gregory Fitz of the Colorado Health Science Center (Denver, Colorado). The cells were grown in minimum essential medium (MEM) (Sigma, St-Louis, Missouri) containing 25 mM sodium bicarbonate, 2 mM glutamine, 5% fetal bovine serum and 1% penicillin-streptomycin equilibrated at 37°C with 5% carbon dioxide/95% oxygen. Cells were used between in-house passages 4 and 10 and were grown for 24 h on round glass coverslips.

Materials: Insulin was prepared as a stock solution of 50 µg/mL in 0.01 N hydrochloric acid and diluted daily from frozen aliquots into standard bath solution. A final concentration of 10 nM was used because this is the lowest dose found to yield near-maximal responses, whether at the level of receptor binding, signal transduction or metabolism in cultured rat hepatocytes, as shown by the authors' laboratory and others (11,18-20). Nystatin was prepared as a stock solution of 100 mg/mL in dimethyl sulphoxide and used at a final concentration of 200 µg/mL in the pipette solution. Fura-2 acetoxymethylester (FURA-2 AM) was purchased from Molecular Probes (Eugene, Oregon). Insulin, nystatin and ionomycin were obtained from Sigma. All other chemicals were of reagent grade.

Patch clamp recording: Membrane currents were measured at room temperature using standard patch clamp recording techniques (21). Coverslips with adhered HTC cells were placed in a plastic perfusion chamber (100 µL trough) set on the stage of an inverted microscope (Olympus IMT-2, Carsen Medical, Markham, Ontario) and single cells were selected for study. Cells were continuously superfused (approximately 2 mL/min) at room temperature with a standard bath solution (Bath standard) containing (in mM): sodium chloride 138, potassium chloride 3.8, magnesium sulphate 1.2, mono potassium phosphate 1.2, calcium chloride 1.8, 4-(2-hydroxyethyl)-1--piperazineethanesulfonic acid (HEPES) 10 (pH 7.4 with sodium hydroxide). An eight-way solenoid valve allowed rapid administration and washout of pharmacological agents and various buffers. Patch pipettes typically exhibited resistances of 4 to 6 MΩ when filled with a standard pipette solution (pipette standard) containing (in mM): potassium chloride 140, magnesium chloride 1.2, ethylene glycol-bis (beta-aminoethylether)-N,N,N',N'-tetra-acetic acid (EGTA) 1, HEPES-KOH 10 (pH 7.35). For ion substitution experiments, the following bathing solutions were used: a potassium-rich solution (potassium-gluconate bath solution) containing (in mM) potassium-gluconate 113.4, potassium chloride 25.4, magnesium sulphate 1.2, mono potassium phosphate 1.2, calcium chloride 5 (to keep ionized calcium near normal in view of the chelating effect of gluconate), HEPES-KOH 10 (pH 7.4); and a nonpermeant cation-rich solution containing (in mM) *N*-methyl-D-glucamine-hydrochloric acid (NMDG-hydrochloric acid) 141.8, magnesium sulphate 1.2, calcium chloride 1.8, HEPES-NMDG 10 (pH 7.4). All bath solutions contained 5 mM glucose and 1 mM pyruvate as energy sources. In these same ion substitution studies, patch pipettes were filled with the following solutions as required: a potassium-rich solution (potassium-gluconate pipette solution) containing (in mM) potassium-gluconate 132.9, potassium chloride 7.1, magnesium chloride 1.2, EGTA 1, HEPES-KOH 10 (pH 7.35); a nonpermeant cation-rich solution containing (in mM) NMDG-hydrochloric acid 140, magnesium chloride 1.2,

EGTA 1, HEPES-NMDG 10 (pH 7.35). All solutions were filtered through 0.22 µm cellulose membranes before use.

Whole cell recordings were carried out using the perforated patch method described by Horn and Marty (22). Briefly, the tip of the pipette was capillary filled with the appropriate pipette solution (approximately 3 s immersion), and the rest of the pipette was then backfilled with the same solution containing nystatin (200 µg/mL). After formation of a seal between the pipette and cell membrane, the membrane potential was held at –40 mV until continuity with the cell interior was fully established (20 to 40 mins), as shown from capacitative transients induced by short 20 mV voltage steps given every 5 mins. Membrane potential was measured in the current clamp (I=0) mode.

After Giga-seal formation, electrical signals were amplified and filtered (3 kHz) with a L/M-EPC-7 patch clamp amplifier (Medical Systems Corp, Greenvale, New York), continuously monitored on an oscilloscope and displayed on a chart recorder. Simultaneously, currents were digitized using a two-channel A/D converter (Instrutech, Elmont, New York) and recorded on standard VHS video magnetic tape. A TL-1 DMA Interface and the PClamp software (v 5.5.1) were used for data acquisition, and PClamp v 6.0 was used for data analysis (Axon Instruments, Foster City, California).

To construct current-voltage (I/V) curves, voltage clamp protocols were used where cells were held at –40 mV (close to the resting potential of HTC cells – see 'Results' section) and stepped from –80 to +60 mV in consecutive 20 mV voltage steps lasting 250 ms each. In all cases presented, I/V relationships were found to be linear with a correlation coefficient greater than or equal to 0.9.

Intracellular calcium measurement: HTC cells were loaded with 1.5 µM Fura-2 AM for 45 mins at room temperature in bicarbonate-free MEM medium. Coverslips with adhered cells were transferred into a 100 µL plastic chamber placed on the stage of an inverted microscope coupled to a spectrofluorimeter (Deltascan RF-D4010, Photon Technology International Inc, London, Ontario). Cells were superfused at a flow rate of 2 to 3 mL/min with standard bath solution (see above) at room temperature. Excitation wavelengths were 350 and 380 nm, while fluorescence emission was measured at 505 nm. Intracellular dye calibration was performed in situ by perfusion of 3.5 µM ionomycin in a solution containing either 4 mM EGTA (Rmin, 350:380 fluorescence ratio in calcium-free solution) or 4 mM calcium chloride (Rmax, 350:380 fluorescence ratio at saturating calcium). The autofluorescence was determined by quenching free FURA acid with 2 mM manganese chloride. Once corrected for autofluorescence, the fluorescence ratios (350:380) were transformed into calcium concentrations, using the OSCAR software supplied by Photon Technology International.

To assess changes in calcium influx, two experimental approaches that were used in many studies (23-26) were selected. The first experimental protocol involved perfusing cells with a solution where extracellular calcium was withdrawn (EGTA chelation) for a period after which normal

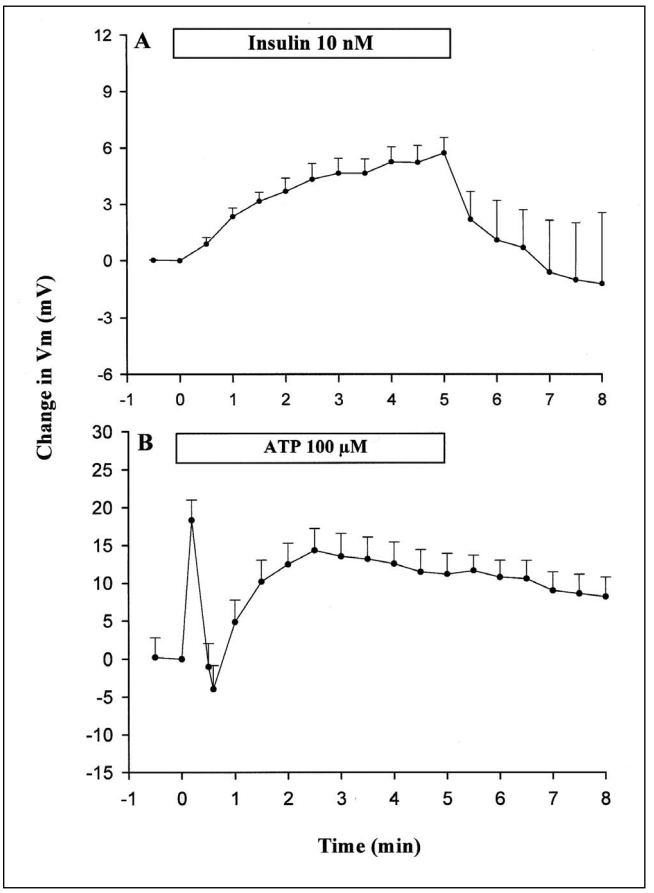

Figure 1) *The effect of 10 nM insulin (A) or of 100 µM ATP (B) on membrane potential in HTC cells. The trace in panel A is a composite graph of the mean ± SEM changes in membrane potential observed in 21 whole-cell experiments for a 5 min administration of insulin and in five such experiments for the return to baseline after removal of the hormone. Panel B presents the mean ± SEM changes in membrane potential observed in 24 whole-cell experiments for a 5 min administration of 100 µM ATP*

external calcium concentrations were restored. The initial rapid rise in cytosolic calcium following readmission of external calcium reflects the entry of calcium from the external environment into the cell. Initial calcium influx rates were assessed by measuring the slope of the calcium-versus-time curve following readmission of external calcium (1.8 mM) after a 13.5 min, calcium-free bathing (0 mM calcium chloride, 4 mM EGTA) period, over the initial 15 s where calcium influx was apparent. The effects of insulin or ATP were determined by relating the measured influx rate to the average value obtained for daily control experiments of calcium withdrawal and readmission, alone.

The second approach used to assess calcium influx into hepatocytes took advantage of the capacity of manganese ions to quench FURA-2 fluorescence. In this case, manganese ions are thought to act as surrogates for calcium ions (27,28). For such FURA-2 fluorescence quenching studies, 50 µM manganese chloride was used and fluorescence signals were monitored at the calcium-insensitive excitation wavelength of 357 nm. The slope of signal

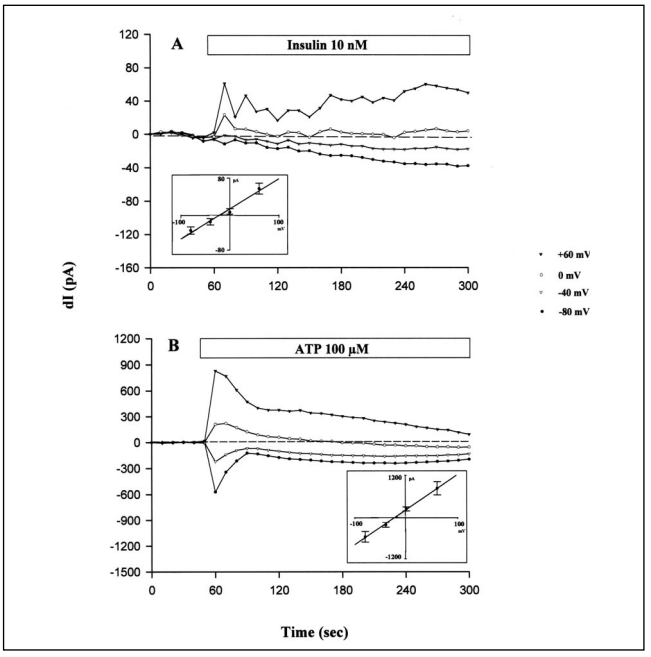

Figure 2) *The effect of 10 nM insulin (***A***) and 100 µM ATP (***B***) on steady-state currents in HTC cells. Curves are the average change in baseline currents induced by insulin (panel A, n=9) and ATP (panel B, n=6) in physiological cationic conditions at –40 mV during a 5 min administration. Insulin-dependent currents measured over the last 50 s of the 5 min administration of the hormone are depicted by the current-voltage (I/V) curve inset in panel A. Agonist-dependent currents recorded at the peak of the initial response induced by ATP (representing cation influx through nonselective channels [29]) are also depicted by the I/V curve inset in panel B. Error bars are not shown in the current-versus-time traces for the sake of clarity, but coefficients of variation for each point did not exceed 20%. dI pA Change in baseline current in picoamperes*

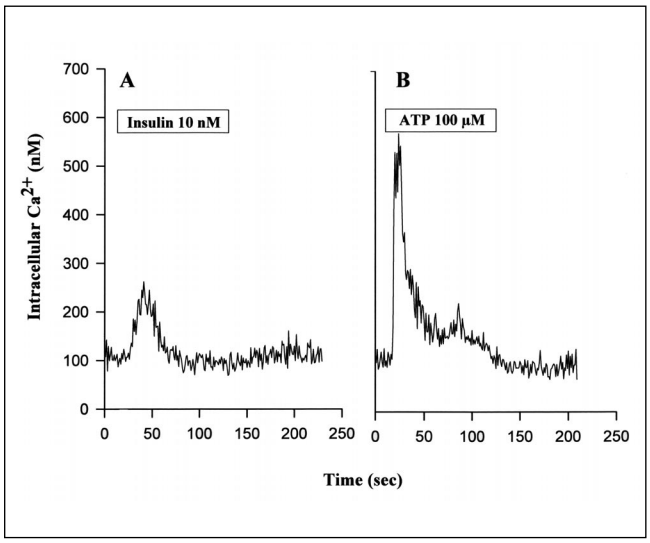

Figure 3) *The effect of 10 nM insulin on intracellular calcium (Ca^{2+}) in physiological cationic conditions. Representative trace of the cytosolic calcium [calcium]i response to 2-min administrations of insulin (10 nM) and ATP (100 µM). Total calcium mobilization (area under the curve over 180 s) was 3.1±0.3 µM (n=25) and 24.9±5.1 µM (n=11) for insulin and ATP, respectively*

quenching obtained (over the first 60 s) with insulin or ATP was related to the control steady-state slope obtained (over the first 60 s) with manganese chloride before their administration. When used, inhibitors were coadministered with manganese chloride and were present throughout the subsequent exposure to insulin.

Statistical analysis: Significant differences between group means were evaluated by ANOVA for independent measures or by paired Students' *t* test as dictated by the experimental protocol.

RESULTS

Effect of insulin on HTC cell membrane potential: Patch clamp experiments were carried out using nystatin-containing pipettes to establish whole-cell recordings by the 'perforated patch technique' (22). In the current clamp mode, the baseline membrane potential of HTC cells averaged –42.9±1.9 mV (n=59). In physiological cationic conditions, insulin (10 nM) induced a slow depolarization that reached an amplitude of 5.7±0.8 mV above baseline (n=21) within 5 mins and was reversible upon removal of the hormone (Figure 1A). In additional experiments, this depolarization remained stable for up to 10 mins of insulin administration (results not shown). This is similar to that observed previously in primary cultures of rat hepatocytes (4). By comparison, ATP (100 µM) induced a typical triphasic response of membrane potential (V_m), as described by Fitz and Sostman (29) (Figure 1B). ATP is a purinergic agonist that acts mainly via G protein-coupled P_{2U} receptors in HTC cells (30) and was used as a positive control for cell responsiveness.

Effect of insulin on steady-state currents in HTC cells: To study the effect of agonists on membrane currents, HTC cells held in the whole cell configuration were perfused with 10 nM insulin or 100 µM ATP for 5 mins. In physiological cationic conditions, administration of insulin induced a small monophasic inward current at resting potential (n=9, Figure 2A). On average, insulin-induced currents exhibited a whole-cell linear slope conductance of 663±100 pS and a reversal potential (E_{rev}) of –17.9 mV (I/V curve inset in Figure 2A). In the same ionic conditions, ATP induced the expected triphasic response (Figure 2B), whose initial part was clearly shown by Fitz and Sostman (29) to be a nonselective cation current. In the present study, such currents had a mean whole-cell linear slope conductance of 10.1±2.3 nS (n=6) and a reversal potential of –21.6 mV (I/V curve inset in Figure 2B).

Because the E_{rev} of insulin-induced currents indicated a possible mixture of potassium, chloride and nonselective cation components, additional experiments were carried out using ion substitutions. The equilibrium potential for potassium ions (E_K) was first moved to 0 mV, and the equilibrium potential for chloride ions (E_{Cl}) to +35 mV (standard pipette solution, potassium-gluconate bath solution, as

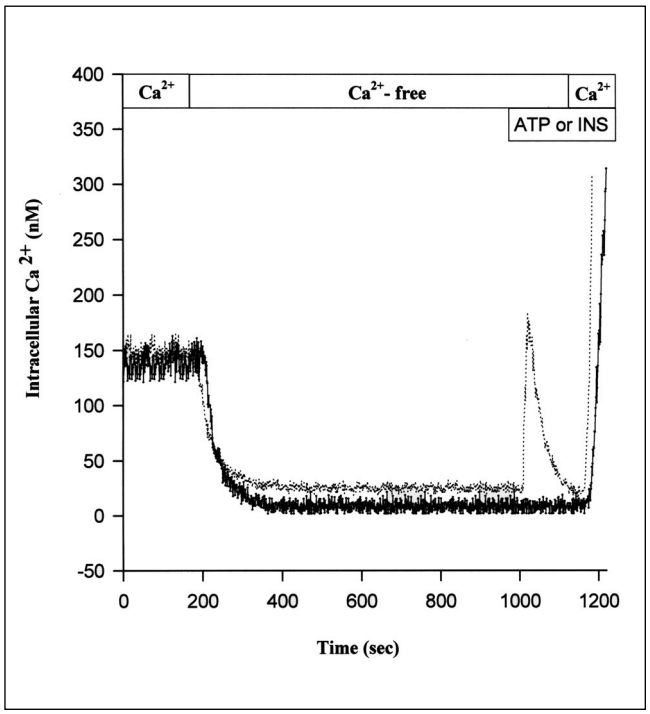

Figure 4) *Effect of insulin on intracellular calcium (Ca_2^+) in calcium-free bathing conditions. Representative traces of the [calcium]i response of HTC cells to 2.5 min administrations of 10 nM insulin (—) or 100 µM ATP (····) after 13.5 mins in standard bath solution lacking calcium chloride to which 4 mM ethylene glycol-bis (beta-aminoethylether)-N,N,N′,N′-tetra-acetic acid (EGTA) was added (calcium free, 'Materials and Methods') The single sharp response induced by ATP (n=16) corresponds to the mobilization of calcium from internal stores, whereas insulin (n=21) failed to elicit a response in the absence of extracellular calcium*

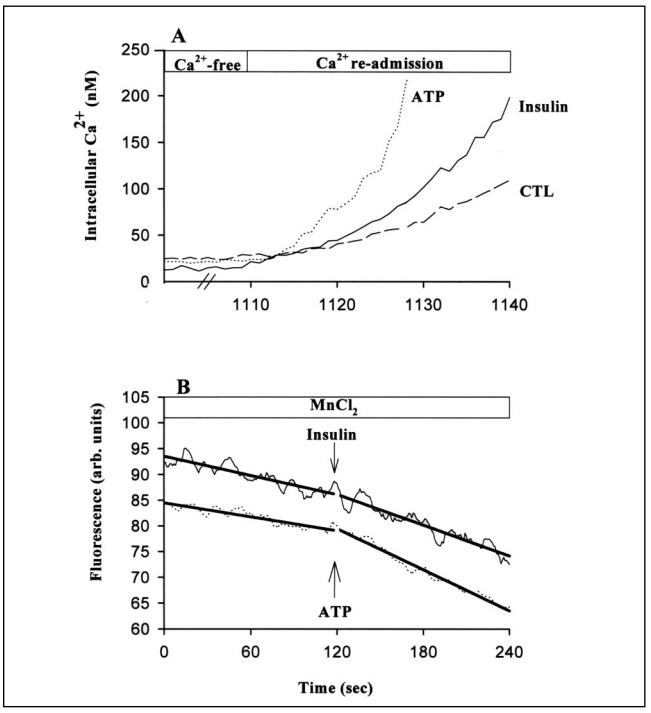

Figure 5) *The effect of 10 nM insulin and 100 µM ATP on the initial calcium (Ca^{2+}) influx rate measured by a protocol of external calcium withdrawal and readmission. After a 13.5 min calcium-free bathing period (see Figure 4), extracellular calcium was reintroduced and an influx of calcium was apparent from the sudden rise in intracellular calcium . Initial calcium influx rates (Vi) were assessed by measuring the slope of the calcium -versus-time curve for the initial 15 s where calcium influx was observed after readmission of external calcium. The effects of insulin (10 nM) or ATP (100 µM) were observed when added for 2.5 mins before calcium readmission. Insulin increased the influx Vi by 1.58-fold (n=21) over a baseline value of 4.65±0.69 nM/s, whereas ATP increased this influx Vi by 2.3-fold (n=16).* **B** *The effect of 10 nM insulin and 100 µM ATP on the basal quench of FURA-2 fluorescence by manganese ions. Manganese chloride (50 µM) was introduced with a calcium-free standard buffer 2 mins before and throughout the subsequent administration of agonists insulin (10 nM) or ATP (100 µM). Insulin increased the quench rate 1.54-fold (n=56), whereas ATP increased this quench rate by 2.16-fold (n=41)(see Materials and Methods). Note different time scale from panel A*

described in 'Materials and Methods'). The reversal potential of the insulin-induced currents shifted to –3 mV, and the slope conductance reached 1030±205 pS (n=8, not significantly different from physiological cationic conditions by unpaired ANOVA). Keeping E_K and the nonselective cation equilibrium potential (E_{cation}) at 0 mV, E_{Cl} was moved to –33 mV (potassium-gluconate bath and pipette solution, as described in 'Materials and Methods'). This yielded an E_{rev} of +8 mV and a mean slope conductance of 776±284 pS for insulin-induced currents (n=6, not significantly different from physiological cationic conditions by unpaired ANOVA). Finally, experiments were performed where all cations were replaced by nonpermeant species (NMDG, 'Materials and Methods'). In such conditions, no current was elicited by insulin administration (data not shown). Collectively, these data suggest that insulin-induced currents are mainly caused by cationic components.

Finally, experiments were carried out in the cell-attached mode. Administration of 10 nM insulin in the medium bathing the cells (n=14) or inclusion of 10 nM insulin in the pipette solution (n=39) never elicited any channel activity. In contrast, bath addition of 100 µM ATP elicited the activation of one to 13 channels in cell-attached patches (n=17), even in cells that failed to respond to insulin. Channel activity was initiated instantly upon ATP administration and returned toward baseline in a pattern resembling cytosolic calcium responses (Figure 3). This response profile as well as channel conductances were similar to those described previously by Fitz and collaborators (30).

Effects of insulin on steady-state intracellular calcium in HTC cell line: When HTC cells were superfused with standard bath solution (see 'Materials and Methods'), the steady-state intracellular calcium concentration averaged 132±9 nM (n=111). Figure 3 presents representative traces of the cytosolic calcium ($[calcium]_i$) responses to 2 mins administration of insulin (10 nM, panel A) or ATP (100 µM, panel B), which acts mainly via a G protein-coupled P_{2U} receptor in these cells (30). As shown, insulin induced a slow

monophasic rise in $[calcium]_i$ compared with the typical biphasic response to the calcium-mobilizing agonist, ATP. These responses were quantified by the area under the curve of the calcium-versus-time relationship. The total intracellular calcium mobilized by insulin amounted to 3.1±0.3 μM (n=25), whereas that induced by ATP was 24.9±5.1 μM (n=11).

To evaluate the role of extracellular calcium in the insulin-induced rise in $[calcium]_i$, experiments were carried out in standard bath solution lacking calcium chloride to which 4 mM EGTA was added. In such calcium-free conditions, the response to 10 nM of insulin (n=21) was not observed, whereas the response to 100 μM of ATP (n=16) was reduced to a single sharp peak as expected from the mobilization of calcium from internal stores (Figure 4). The lack of response to insulin in such calcium-free conditions was not caused by a change in receptor occupancy as confirmed by displacement studies with ^{125}I-insulin (data not shown). These results suggest that insulin induces an influx of external calcium into HTC cells. To verify this, the two different approaches described in 'Materials and Methods' were used. The first consists of extracellular calcium withdrawal and readmission as depicted in Figure 4. After a calcium-free period of 13.5 mins, the initial slope of the rise in $[calcium]_i$ upon calcium readmission was 4.65± 0.69 nM/s, and this was increased 1.58±0.26-fold (n=21, $P<0.05$ by paired *t* test) with the prior administration of 10 nM insulin (Figure 5). ATP (100 μM), which had induced depletion of internal stores as depicted in Figure 4, also induced a statistically significant increase in the initial slope of calcium influx that amounted to 2.3±0.4-fold of the respective daily control (n=16, $P<0.002$ by paired *t* test, Figure 5A).

Another approach, which reflects unidirectional calcium influx pathways, is to measure the rate of FURA-2 quenching induced by manganese ions, which act as surrogates for calcium ions (27,28). During the first minute of administration of 50 μM manganese chloride, the rate of fluorescence quenching was 8.1±0.5 arbitrary units/s (n=103), and this baseline rate was subsequently increased by 1.54±0.08 (n=56) and 2.16±0.33 (n=41)-fold after the addition of 10 nM insulin and 100 μM ATP, respectively (Figure 5B, $P<0.0001$ by paired *t* test in both cases). Collectively, these results support the interpretation that insulin induces calcium influx into HTC cells.

Effects of calcium channel inhibitors on insulin-induced increase in calcium influx: To determine the pharmacological profile of the calcium influx in HTC cells, several inhibitors known to interfere with calcium entry pathways were administered using the manganese quench protocol. Inhibitors were introduced with a calcium-free standard buffer at the same time as 50 μM manganese chloride. First, the divalent cations zinc, cobalt and nickel were tested. Administration of zinc blocked the basal rate of manganese influx, whereas cobalt and nickel ions by themselves were found to quench FURA-2 fluorescence at the monitored calcium-insensitive wavelength of 357 nm (data not shown). Consequently, the data using these divalent cations could not be interpreted. Second, 100 μM verapamil was used, which is a known blocker of voltage-operated calcium channels (31). In the presence of verapamil, insulin accelerated basal manganese influx rate by 1.42±0.1-fold (n=10), which was not statistically different from the effect of insulin alone (not significant by unpaired ANOVA). Then, gadolinium was used, an ion of the lanthanide series known to block calcium entry pathways triggered by the depletion of intracellular calcium pools in cultured hepatocytes (17) and to inhibit nonselective cation channels in hepatoma cells (32). At a concentration of 100 μM, gadolinium prevented insulin from increasing the basal manganese influx rate (1.05±0.09-fold increase, n=25, $P<0.05$ compared with insulin alone by unpaired ANOVA). Finally, 10 μM SKF96365, a compound known to interfere with receptor-operated calcium inflow in rat hepatocytes (23), also abolished the effect of insulin on basal manganese influx rate (0.65±0.08-fold increase, n=12, $P<0.05$ compared with insulin alone by unpaired ANOVA). Neither gadolinium, SKF96365, nor verapamil had a significant effect on the steady-state baseline manganese-induced quench rate (not significant by unpaired ANOVA).

DISCUSSION

The present study shows clearly that insulin causes a small inward current in HTC liver cells maintained near the resting membrane potential in physiological cationic conditions. This insulin-induced current triggers a gradual depolarization of 5.7 mV. Such a slow depolarizing effect of insulin was observed previously following impalements of cultured rat hepatocytes with glass microelectrodes (4), but the underlying currents were not well defined. In the present study, we used ion substitutions to clarify the ionic components of the insulin-induced currents. In physiological cationic conditions, insulin-induced whole-cell currents have an average linear slope conductance of 663 pS and a reversal potential of –17.9 mV, located between the equilibrium potential for potassium ions, on one hand, and that for cations or chloride, on the other. Collapsing the potassium gradient brought the reversal potential of insulin-induced currents close to 0 mV, whereas moving E_{Cl} to +35 or –33 mV did not drive the reversal potential toward more positive or more negative values. In addition, no current was elicited by insulin administration when chloride ions were the major conducting ion species (all cations replaced by a nonpermeant species such as NMDG). These data strongly suggest that insulin-induced inward currents into HTC cells are mainly related to nonselective cationic components.

However, our results also suggest that insulin may induce a small parallel increase in potassium conductance as indicated by the reversal potential obtained in physiological cationic solutions (between E_K and E_{cation}). This conductive pathway may be related to the insulin-induced increase in intracellular calcium discussed below. Indeed, purinergic agonists such as ATP are known to trigger calcium-sensitive potassium currents in HTC cells (29), and calcium-activated potassium channels of small size have already been described in these cells by Lidofsky (33). Such channels could be a putative source of the potassium-selective component induced by insulin that drives the equilibrium potential of

insulin-induced currents partially away from 0 mV (nonselective cation equilibrium potential) in our physiological cationic conditions.

Nonetheless, our results indicate that the major action of insulin is to trigger inward cationic currents in HTC cells that consist principally of a nonselective component that probably contributes to the observed depolarization of HTC cell membrane potential and rise in cytosolic calcium.

Indeed, in the present study, insulin was found to trigger an increase in HTC intracellular calcium that was generally monophasic and transient in nature. This corresponds to what we have recently described in primary rat hepatocytes (11). Similar to the latter study, the insulin-induced changes in hepatocellular calcium were absent when external calcium was chelated, in the present study. This effect was not related to altered insulin receptor occupancy, as confirmed by ^{125}I insulin displacement studies, or to the depletion of internal calcium stores, as shown by the preserved response to the G-coupled purinergic receptor agonist ATP. These results strongly suggest that insulin triggers an influx of external calcium into HTC cells in a manner similar to that found in primary hepatocytes (11).

Further experiments were thus carried out to characterize better the pathways of calcium entry stimulated by insulin in HTC cells. In rat hepatocytes, calcium influx has commonly been estimated either by the manganese quench method or by a protocol of external calcium withdrawal and readmission (23-26). By each of these respective approaches, insulin induced a statistically significant increase of 1.54- and 1.58-fold in the rate of external calcium influx. By comparison, the influx triggered by the purinergic agonist ATP amounted to 2.2- and 2.3-fold over control baseline values, for manganese quench and calcium withdrawal and readmission, respectively. When probed with several calcium channel blockers, the insulin-induced calcium influx (acceleration of manganese quench rate) was inhibited by gadolinium and SFK96365, whereas verapamil was without effect. This is similar to the results obtained recently with primary rat hepatocytes using a different approach (11). In that study, insulin-induced calcium responses were inhibited by nickel and gadolinium, but not by verapamil. As mentioned earlier, nonselective cation channels in HTC cells were also shown to be sensitive to nickel and SFK96365, but not to verapamil (16). Such nonselective cation channels could thus be one of the molecular targets of insulin action on hepatocellular membrane conductance.

However, we were unable to observe direct activation of such channel activity in cell-attached recordings, whether insulin was introduced in the bathing or pipette solution. Positive control experiments with the P_{2U} purinergic agonist ATP confirmed that nonselective channels were indeed present in our HTC cells and responded as previously reported by Fitz et al (30). In view of the reported single-channel conductances of 18 and 28 pS for the two types of nonselective cation channels described in HTC cells, and of the small peak amplitude of insulin-induced inward currents (663 pS whole-cell slope conductance), we would expect insulin to activate at most 24 to 37 such channels per cell. Hence, it is not surprising that direct activation of single-channel activity could not be observed with insulin in cell-attached patches. In comparison, ATP activated a whole-cell linear slope conductance of 10.1 nS, which corresponds to the activation of 360 to 561 of the channels mentioned above. This is consistent with the responses involving one to 13 channels (average of 5.3±0.7 channels, n=17) that we could successfully and reproducibly observe in cell-attached patches with ATP. In contrast, the chance of isolating under the patch pipette one or more of the 24 to 37 channels activated per cell with insulin as the agonist was very slim. This holds particularly true if close proximity between the insulin receptor and the channels is required for activation. Further experiments will be required to address this question.

Nevertheless, our results show clearly that HTC cells are an appropriate model in which to study further the molecular targets of insulin action at the level of liver cell membrane conductance as well as the coupling mechanisms with the insulin receptor. Indeed, evidence from several laboratories supports this notion. First, as mentioned, these cells possess nonselective cation channels very similar to those present on primary hepatocytes (30). HTC cells also exhibit volume-sensitive increases in membrane chloride (34) and sodium (35) fluxes, as do normal hepatocytes (36,37). Secondly, the HTC liver cell line has successfully been used to characterize several components of insulin receptor signalling cascades (38,39). Notably, insulin-induced stimulation of glycogen synthesis in HTC cells (40,41), as in primary hepatocytes (42,43), was found to implicate phosphatidylinositol-3-kinase. Most interestingly, this signalling pathway (19), as well as that involving mitogen-activated protein (MAP) kinase (11), were shown clearly by our laboratory to require insulin-induced calcium influx for their full expression in rat hepatocytes. Finally, we found recently that insulin also stimulates $p^{44/42}$ MAP kinase activity in HTC cells (44). When external calcium was chelated by 4 mM EGTA, the stimulation of $p^{44/42}$ MAP kinase activity by 10 nM insulin was reduced by 50% (44). This strongly indicates that calcium influx in HTC cells, like that in primary hepatocytes, plays a physiological role in mediating a significant portion of insulin action.

CONCLUSIONS

Our results demonstrate clearly that HTC cells respond to insulin with inward cationic currents and that nonselective cation currents are the principal source of insulin-induced cation influx. This action causes a depolarization of membrane potential and is associated with an increased influx of extracellular calcium through gadolinium- and SKF96365-sensitive but verapamil-insensitive pathways. The present study thus supports the notion that cation influx is an important component of insulin action in liver cells.

ACKNOWLEDGEMENTS: We thank Ms Kenza Benzeroual for the $p^{44/42}$ MAP kinase assays and for helpful discussion.

REFERENCES

1. Ullrich A, Schlessinger J. Signal transduction by receptor tyrosine kinase activity. Cell 1990;60:755-65.
2. Kraus-Friedmann N. Hormonal regulation of hepatic gluconeogenesis. Physiol Rev 1984;64:170-258.
3. Lawrence JC Jr. Signal transduction and protein phosphorylation in the regulation of cellular metabolism by insulin. Annu Rev Physiol 1992;54:177-93.
4. Wondergem R. Insulin depolarization of rat hepatocytes in primary monolayer culture. Am J Physiol 1983;244:C17-23.
5. Friedmann N, Dambach G. Antagonistic effect of insulin on glucagon-evoked hyperpolarisation: A correlation between changes in membrane potential and gluconeogenesis. Biochim Biophys Acta 1980;596:180-5.
6. Agius L, Peak M, Beresford G, et al. The role of ion content and cell volume in insulin action. Biochem Soc Trans 1994;22:516-22.
7. Touyz RM, Schiffrin EL. Insulin-induced Ca2+ transport is altered in vascular smooth muscle cells of spontaneously hypertensive rats. Hypertension 1994;23:931-5.
8. Klip A, Li G, Logan WJ. Role of calcium ions in insulin action on hexose transport in L6 muscle cells. Am J Physiol 1984;247:E297-304.
9. Blackmore PF, Augert G. Effects of hormones on cytosolic free calcium in adipocytes. Cell Calcium 1989;10:561-7.
10. Draznin B, Kao M, Sussman KE. Insulin and glyburide increase cytosolic free-Ca2+ concentration in isolated rat adipocytes. Diabetes 1987;36:174-8.
11. Benzeroual K, Van de Werve G, Meloche S, et al. Insulin induces Ca2+ influx into isolated rat hepatocytes couplets. Am J Physiol 1997;272:G1425-32.
12. Mauger JP, Claret M. Calcium channels in hepatocytes. J Hepatol 1988;7:278-82.
13. Hughes BP, Both K, Harland L, et al. Identification of an mRNA species which encodes a voltage-operated Ca2+ channel in rat liver. Biochem Mol Biol Int 1993;31:193-200.
14. Lidofsky SD, Xie MH, Sostman A, et al. Vasopressin increases cytosolic sodium concentration in hepatocytes and activates calcium influx through cation-selective channels. J Biol Chem 1993;268:14632-6.
15. Lidofsky SD, Sostman A, Fitz JG. Regulation of cation-selective channels in liver cells. J Membr Biol 1997;157:231-6.
16. Lidofsky SD. Properties of hepatocellular cation-selective channels suggest a prominent role in receptor-mediated calcium entry. Hepatology 1995;22:306A. (Abst)
17. Fernando KC, Barritt GJ. Characterisation of the divalent cation channels of the hepatocyte plasma membrane receptor-activated Ca2+ inflow system using lanthanide ions. Biochim Biophys Acta 1995;1268:97-106.
18. Morin O, Fehlmann M, Freychet P. Binding and action of insulin and glucagon in monolayer cultures and fresh suspensions of rat hepatocytes. Mol Cell Endocrinol 1982;25:339-52.
19. Benzeroual K, Pandey S, Srivastava A, et al. Insulin-induced Ca2+ entry in hepatocytes is important for PI 3-kinase activation, but not for insulin receptor and IRS-1 tyrosine phosphorylation. Biochim Biophys Acta 2000;1495:14-23.
20. Iynedjian PB, Jotterand D, Nouspikel T, et al. Transcriptional induction of glucokinase gene by insulin in cultured liver cells and its repression by the glucagon-cAMP system. J Biol Chem 1989;264:21824-9.
21. Hamill OP, Marty A, Neher E, et al. Improved patch clamp techniques for high resolution current recording from cells and cell-free membrane patches. Pfluegers Arch 1981;391:85-100.
22. Horn R, Marty A. Muscarinic activation of ionic currents measured by a new whole-cell recording method. J Gen Physiol 1988;92:145-59.
23. Fernando KC, Barritt GJ. Characterisation of the inhibition of the hepatocyte receptor-activated Ca2+ inflow system by gadolinium and SK&F 96365. Biochim Biophys Acta 1994;1222:383-9.
24. Kass GEN, Llopis J, Chow SC, et al. Receptor-operated calcium influx in rat hepatocytes: Identification and characterization using manganese. J Biol Chem 1990;265:17486-92.
25. Glennon MC, Bird GSJ, Kwan C-Y, et al. Actions of vasopressin and the Ca2+-ATPase inhibitor, thapsigargin, on Ca2+ signaling in hepatocytes. J Biol Chem 1992;267:8230-3.
26. Barritt GJ, Hughes BP. The nature and mechanism of activation of the hepatocyte receptor-operated Ca2+ inflow system. Cell Signal 1991;3:283-92.
27. Parekh AB, Penner R. Store depletion and calcium influx. Physiol Rev 1997;77:901-30.
28. Crofts JN, Barritt GJ. The liver cell plasma membrane Ca2+ inflow systems exhibit a broad specificity for divalent metal ions. Biochem J 1990;269:579-87.
29. Fitz JG, Sostman AH. Nucleotide receptors activate cation, potassium and chloride currents in a liver cell line. Am J Physiol 1994;266:G544-53.
30. Fitz JG, Sostman AH, Middleton JP. Regulation of cation channels in liver cells by intracellular calcium and protein kinase C. Am J Physiol 1994;266:G677-G684.
31. Triggle DJ. Calcium-channel drugs: Structure-function relationships and selectivity of action. J Cardiovasc Pharmacol 1991;18 (Suppl 10):S1-6.
32. Bear C, Li C. Calcium-permeable channels in rat hepatoma cells are activated by extracellular nucleotides. Am J Physiol 1991;261:C1018-24.
33. Lidofsky SD. Convergent and parallel activation of low-conductance potassium channels by calcium and cAMP-dependent protein kinase. Proc Natl Acad Sci USA 1995;92:7115-9.
34. Roman RM, Bodly KO, Wang Y, et al. Activation of protein kinase C alpha couples cell volume to membrane Cl- permeability in HTC hepatoma and Mz-ChA-1 cholangiocarcinoma cells. Hepatology 1998;28:1073-80.
35. Schlenker T, Feranchak AP, Schwake I, et al. Functional interactions between oxidative stress, membrane Na+ permeability, and cell volume in rat hepatoma cells. Gastroenterology 2000;118:395-403.
36. Haddad P, Graf J. Volume-regulatory K+ fluxes in the isolated perfused rat liver: characterization by ion transport inhibitors. Am J Physiol 1989;257:G357-63.
37. Haddad P, Beck JS, Boyer JL, et al. Role of chloride ions in liver cell volume regulation. Am J Physiol 1991;261:G340-8.
38. Band CJ, Posner BI. Phosphatidylinositol 3-kinase and p 70S6k are required for insulin but not bisperoxovanadium 1,10-phenanthroline (bpVphen) inhibition of insulin-like growth factor binding protein gene expression. J Biol Chem 1997;272:138-45.
39. Sung CK, Sanchez-Margalet V, Goldfine ID. Role of p85 subunit of phosphatidylinositol-3-kinase as an adaptor molecule linking the insulin receptor, p62, and GTPase-activating protein. J Biol Chem 1994;269:12503-7.
40. Sung CK, Chol WS, Sculla P. Insulin-stimulated glycogen synthesis in cultured hepatoma cells: differential effects of inhibitors of insulin signaling molecules. J Recept Signal Transduct Res 1998;18:243-63.
41. Sanchez-Margalet V. Stimulation of glycogen synthesis by insulin requires S6 kinase and phosphatidylinositol-3-kinase in HTC-IR cells. J Cell Physiol 2000;182:182-8.
42. Carlsen J, Christiansen K, Vinten J. Insulin stimulated glycogen synthesis in isolated rat hepatocytes: Effects of protein kinase inhibitors. Cell Signal 1997;9:447-50.
43. Lavoie L, Band CJ, Kong M, et al. Regulation of glycogen synthase in rat hepatocytes – Evidence for multiple signaling pathways. J Biol Chem 1999;274:28279-85.
44. Benzeroual K, Vallerand D, Mathé L, et al. Interaction between insulin and purinergic agonist ATP at the level of membrane potential, cytosolic calcium and MAP kinase in the HTC liver cell line. Hepatology 1999;30:403A. (Abst)